Electronic Supplementary Material (ESI) for Journal of Materials Chemistry C.

Supporting Information

Reduced graphene oxide on perovskite solar cells: the influence on film formation, photophysics, performance, and stability

Paulo Ernesto Marchezi[1], Francineide Lopes de Araújo[1], Rodrigo Szostack[1], José Carlos Germino[1], Eralci M. Therézio[2], Alexandre Marletta[3] and Ana Flavia Nogueira[1]*

[1] University of Campinas (UNICAMP), Laboratório de Nanotecnologia e Energia Solar, Chemistry Institute, Campinas, PO Box 6154, 13083-970, Brazil.
[2] Physics Institute, Federal University of Mato Grosso, Cuiabá, Brazil.
[3] Physics Institute, Federal University of Uberlândia, Uberlândia, Brazil

* Correspondence: anafla@unicamp.br

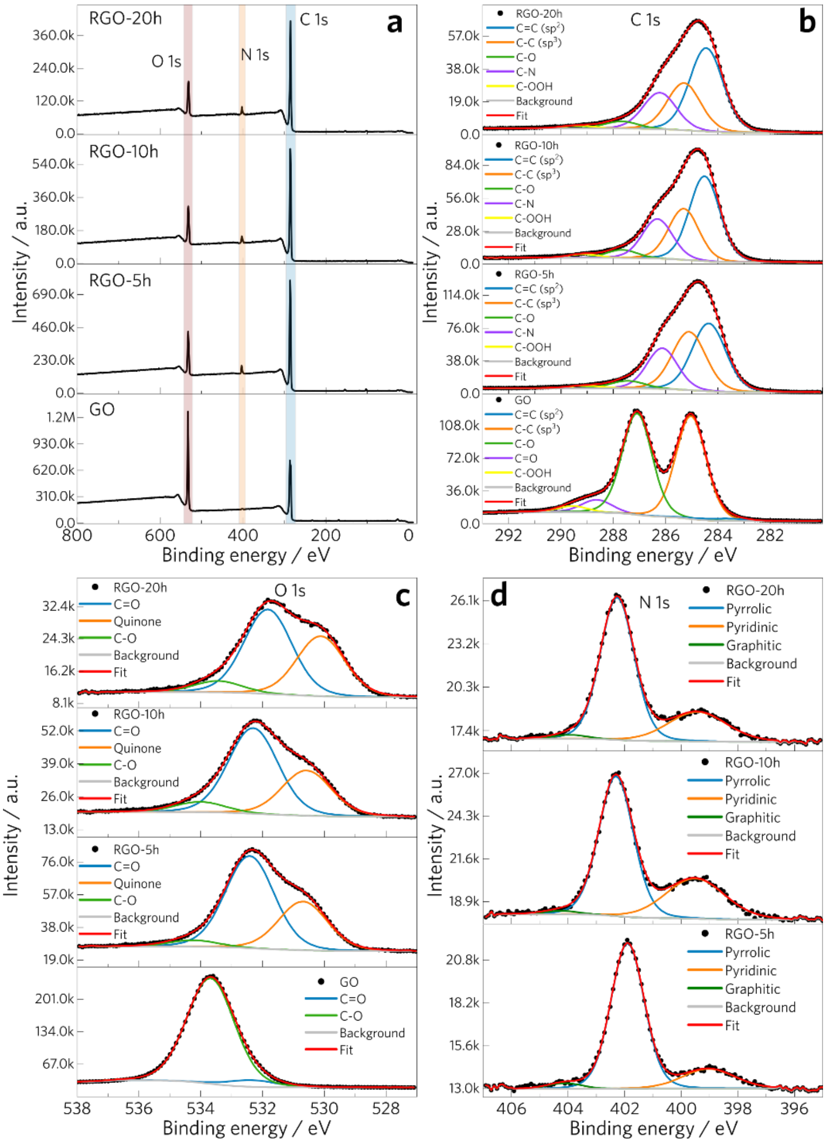

Figure S1: High resolution XPS analysis. (a) Survey XPS spectra for GO, RGO-5h, RGO-10h and RGO-20h. (b) C 1s high resolution XPS core-level spectra of all samples; deconvolution peaks are attributed to C=C (blue), C-C (orange), C-O (green), C-N (purple) and C-OOH (yellow). (c) O 1s high resolution XPS core-level spectra of all samples; deconvolution peaks are attributed to quinone (orange), C=O (blue) and C-O (green). (d) N 1s high resolution XPS core-level spectra of all samples; deconvolution peaks are attributed to pyridinic (orange), pyrrolic (blue), and graphitic (green).

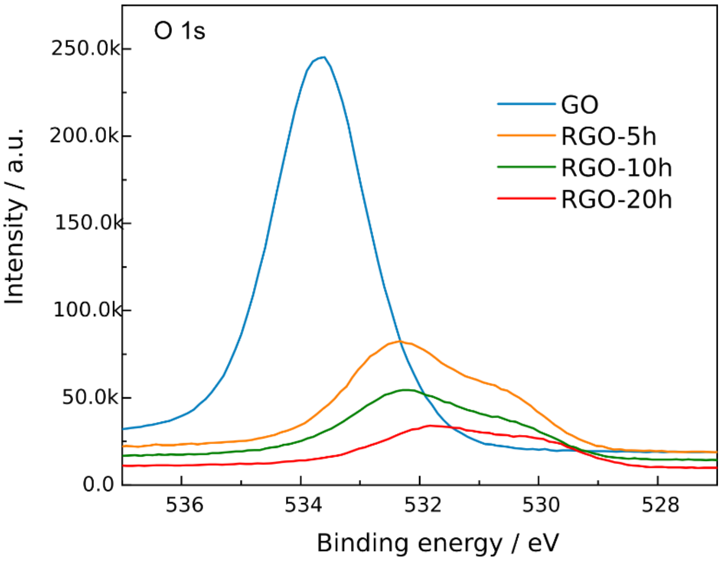

Figure S2: O 1s high resolution XPS core-level spectra of all samples.

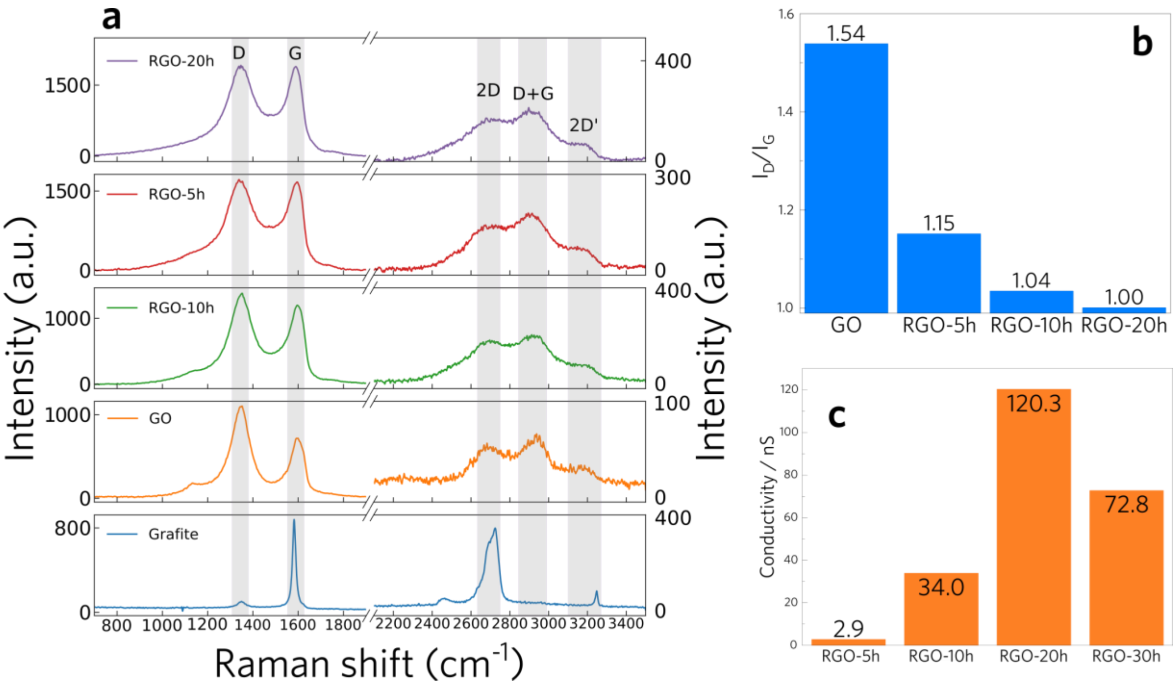

Figure S3: Raman spectra for GO and all RGO synthesized in this work (a), ID/IG ratios (b) and conductivity of the RGO films (c).

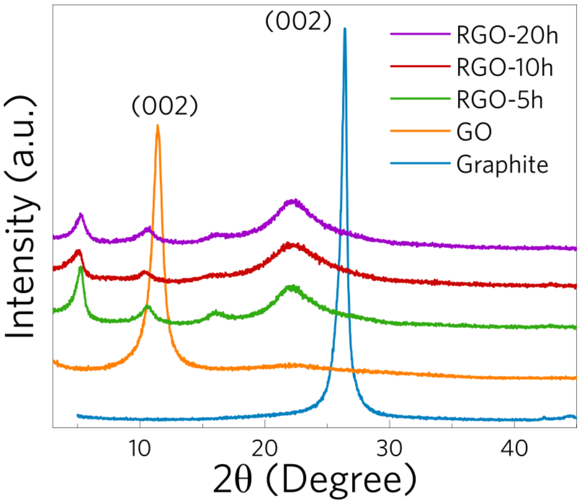

Figure S4:XRD measured for graphite, GO and all RGO used in this work.

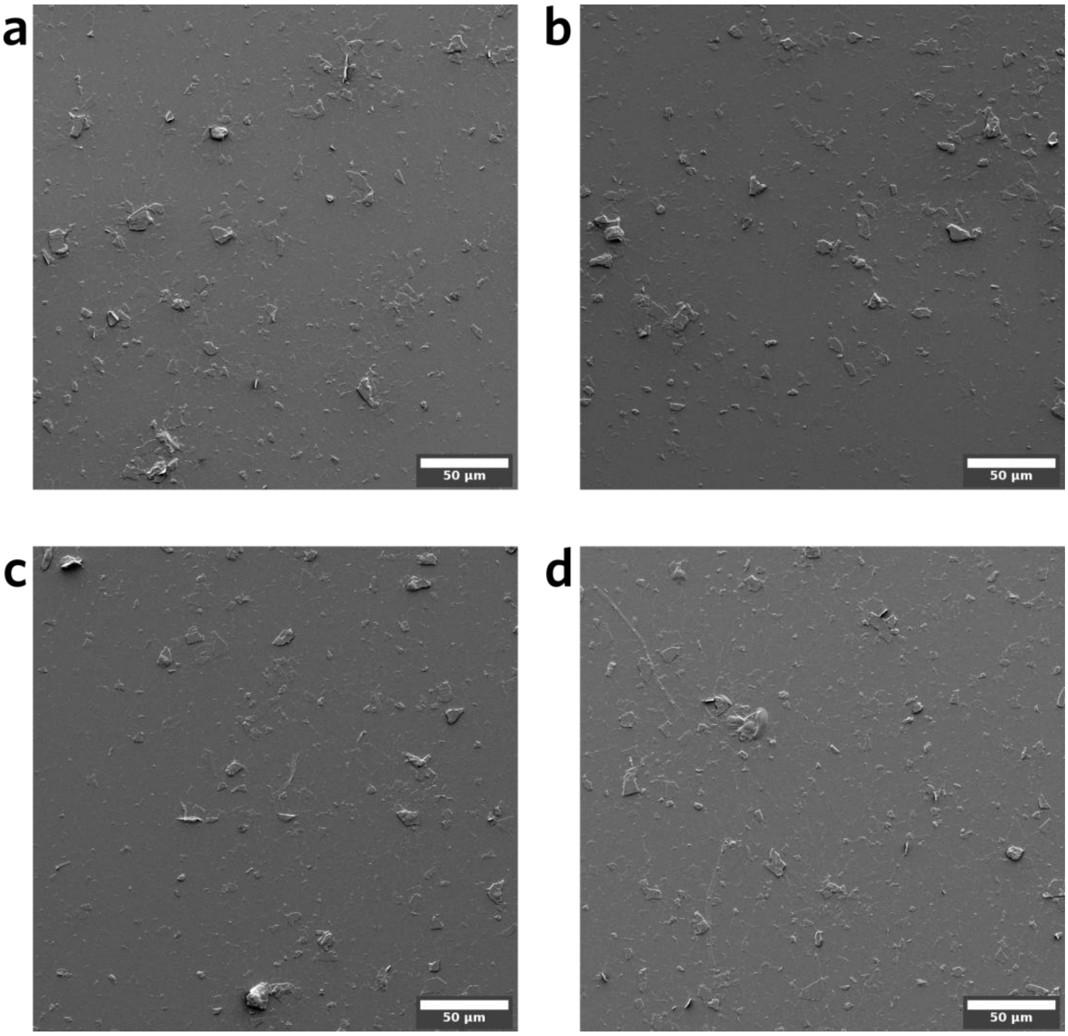

Figure S5: SEM images of GO (a), RGO-5h (b), RGO-10h and RGO-20h.

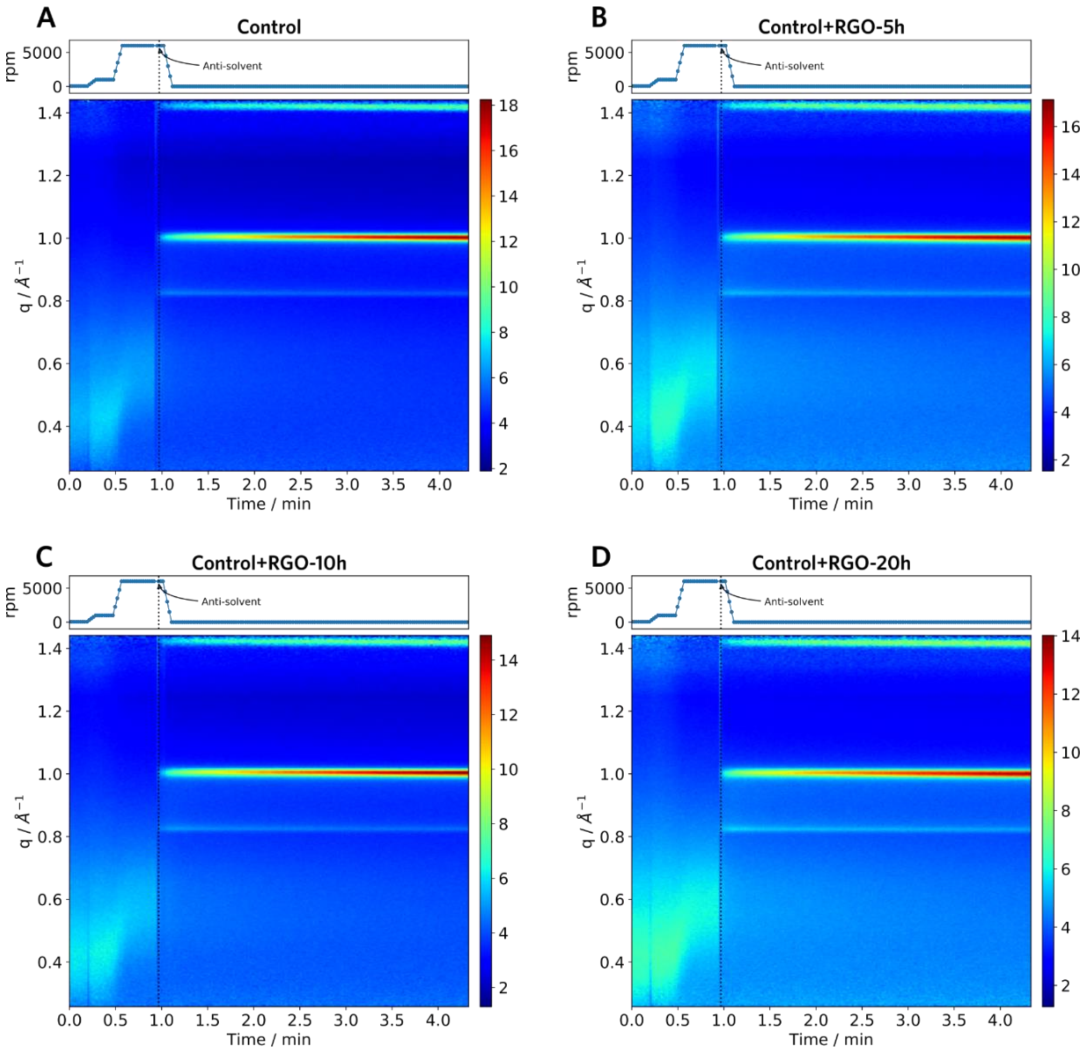

Figure S6: GIWAXS diffractogram map over time along the spin-coating conditions during the measurements of the Control (A), Control+RGO-5h (B), Control+RGO-10h (C), and Control+RGO-20h (D).

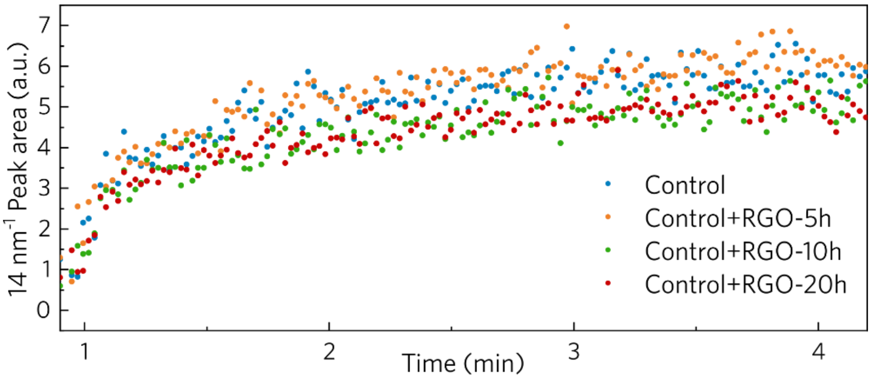

Figure S7: Area of q = 14 nm^{-1} peak over time.

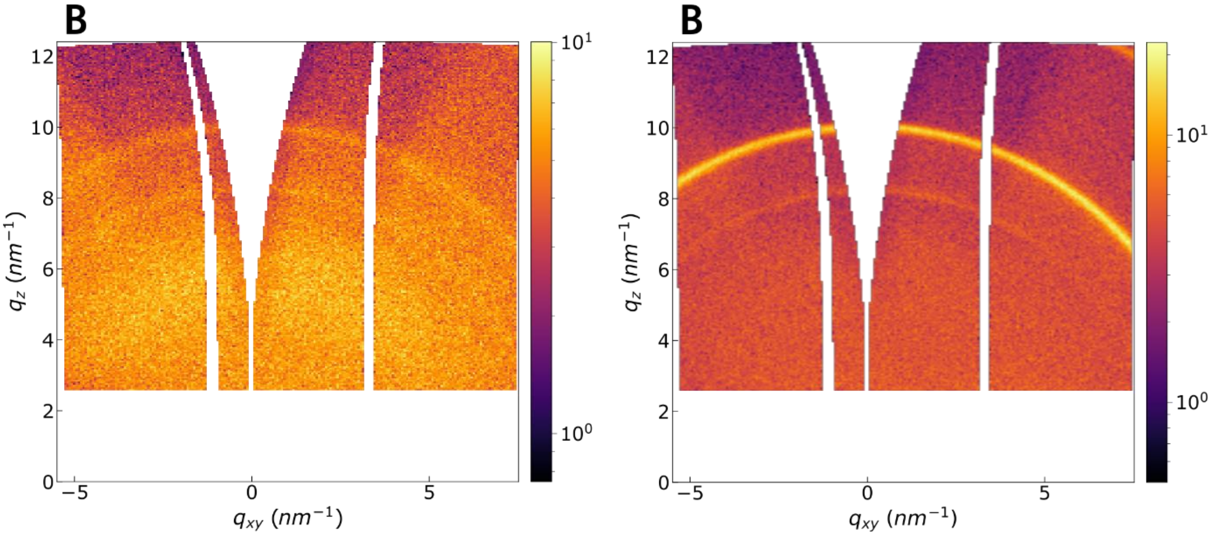

Figure S8: Control sample GIWAXS reciprocal lattice maps (first (A) and last (B) measures) related to the 1D profiles in Figure S5A and Figure 2.

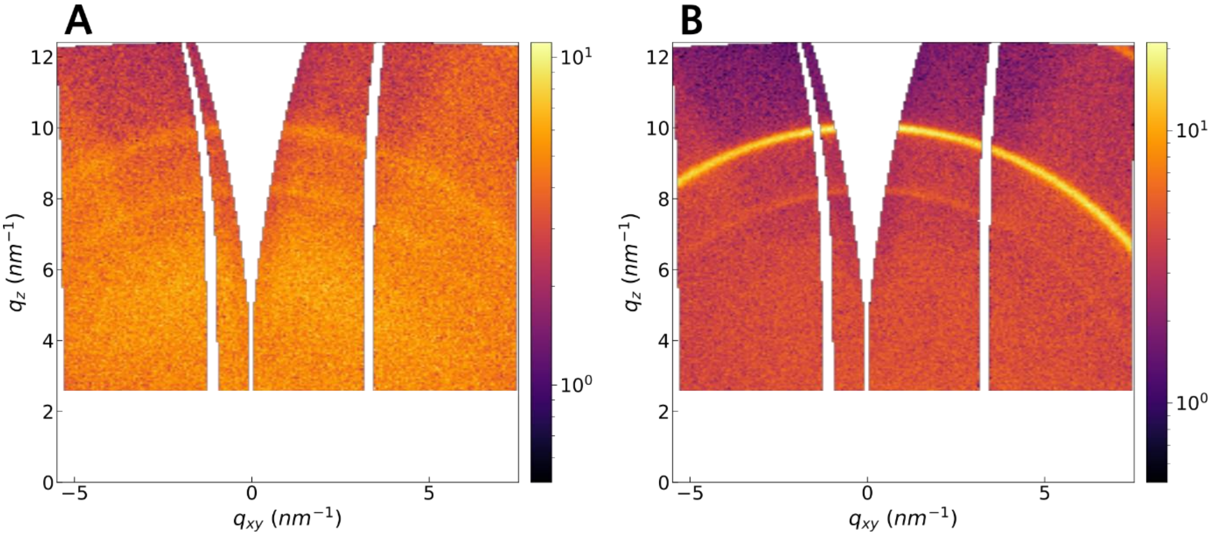

Figure S9: Control+RGO-5h sample GIWAXS reciprocal lattice maps (first (A) and last (B) measures) related to the 1D profiles in Figure S5B and Figure 2.

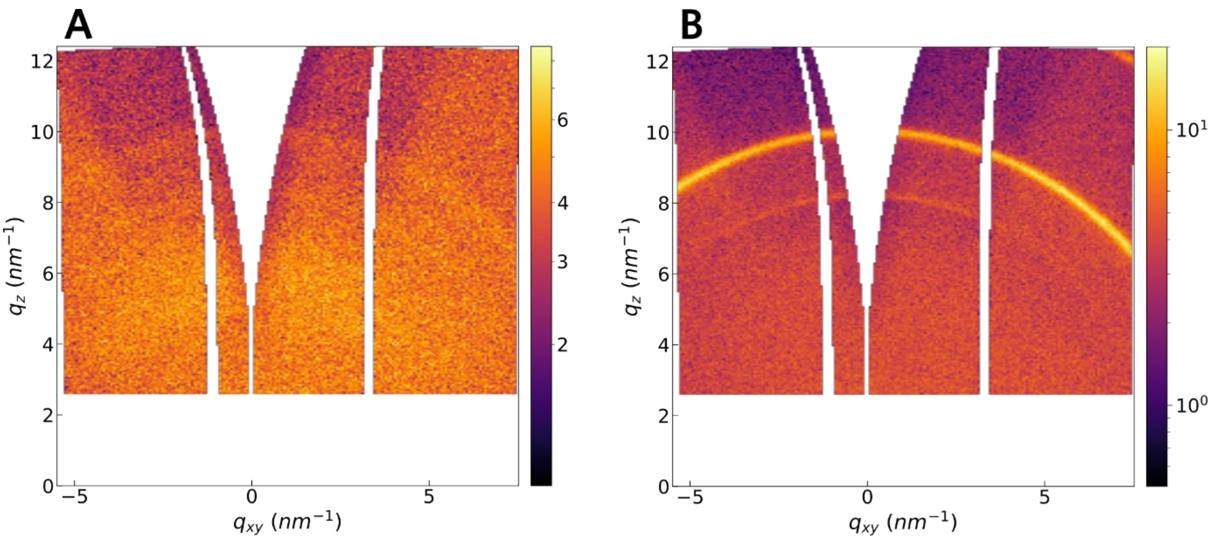

Figure S10: Control+RGO-10h sample GIWAXS reciprocal lattice maps (first (A) and last (B) measures) related to the 1D profiles in Figure S5C and Figure 2.

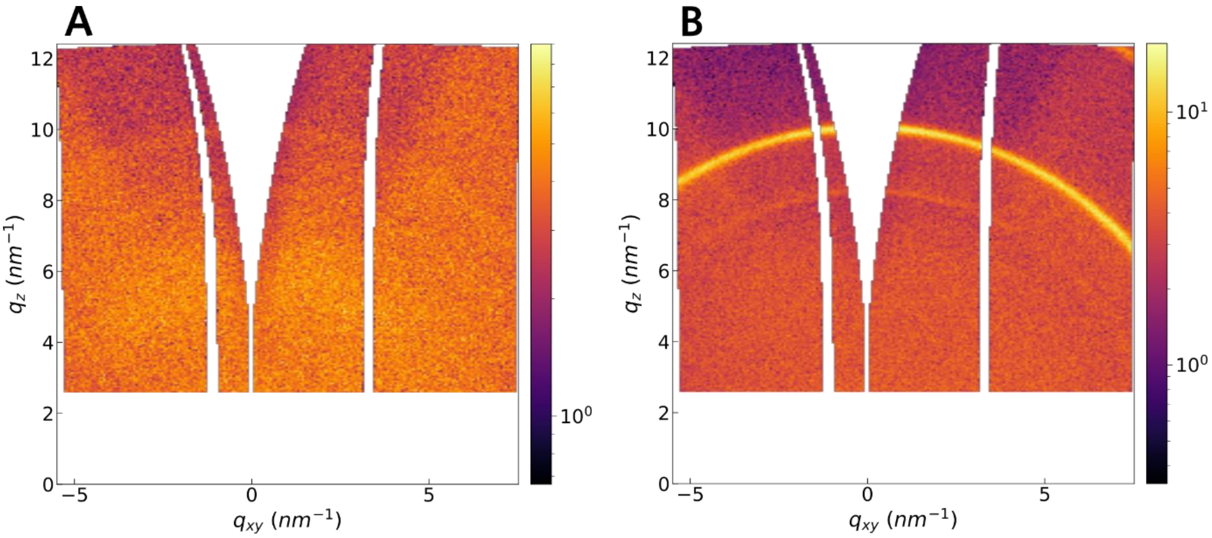

Figure S11: Control+RGO-20h sample GIWAXS reciprocal lattice maps (first (A) and last (B) measures) related to the 1D profiles in Figure S5D and Figure 2.

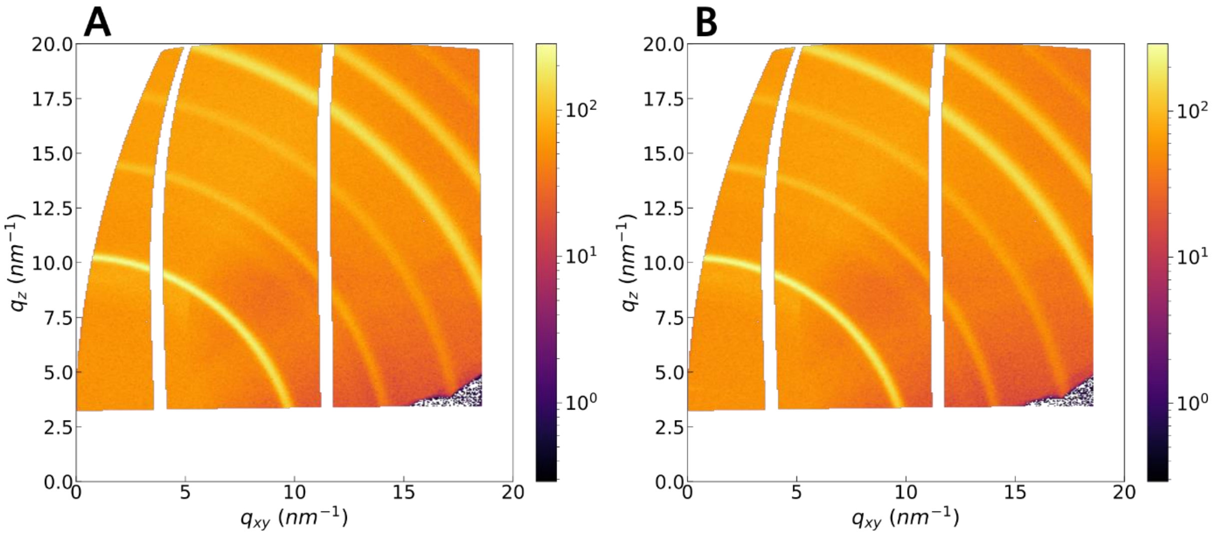

Figure S12: Control sample GIWAXS reciprocal lattice maps (first (A) and last (B) measures) related to the 1D profiles in Figure 3.

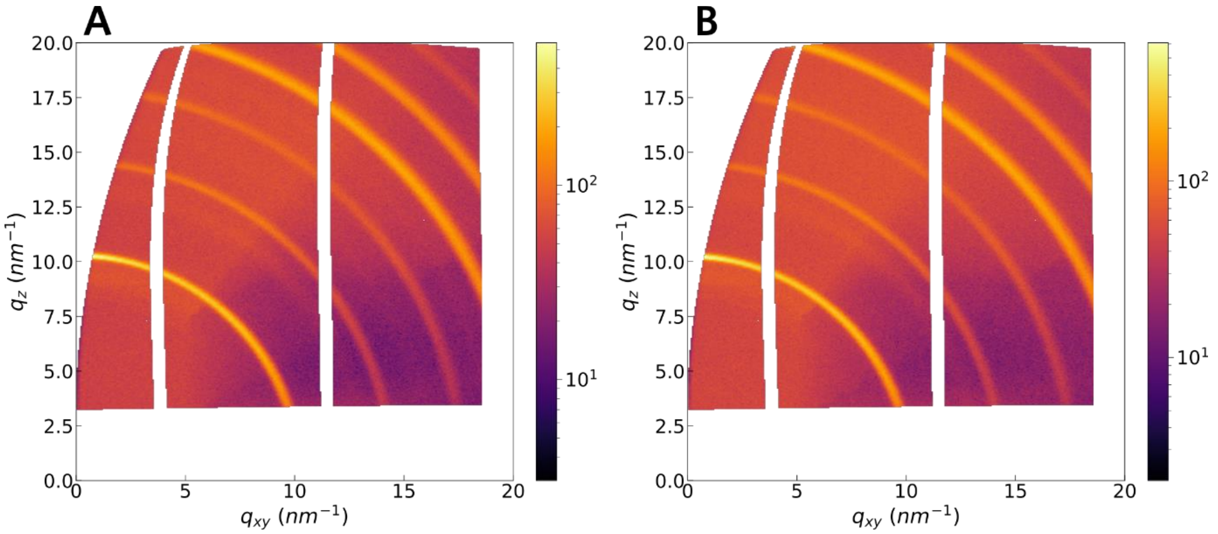

Figure S13: Control+RGO5h sample GIWAXS reciprocal lattice maps (first (A) and last (B) measures) related to the 1D profiles in Figure 3.

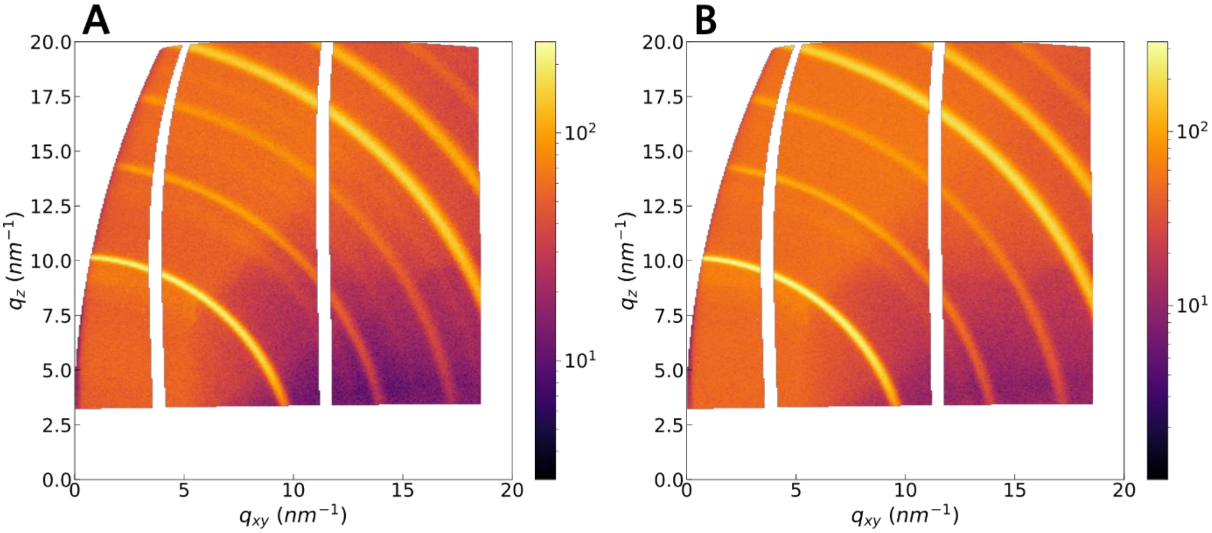

Figure S14: Control+RGO10h sample GIWAXS reciprocal lattice maps (first (A) and last (B) measures) related to the 1D profiles in Figure 3.

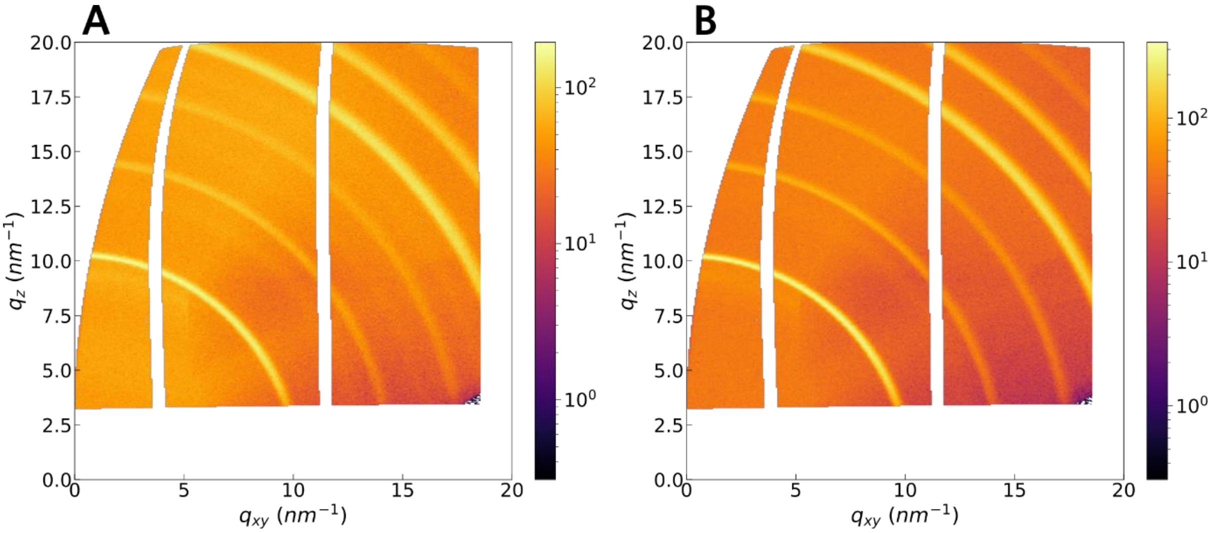

Figure S15: Control+RGO20h sample GIWAXS reciprocal lattice maps (first (A) and last (B) measures) related to the 1D profiles in Figure 3.

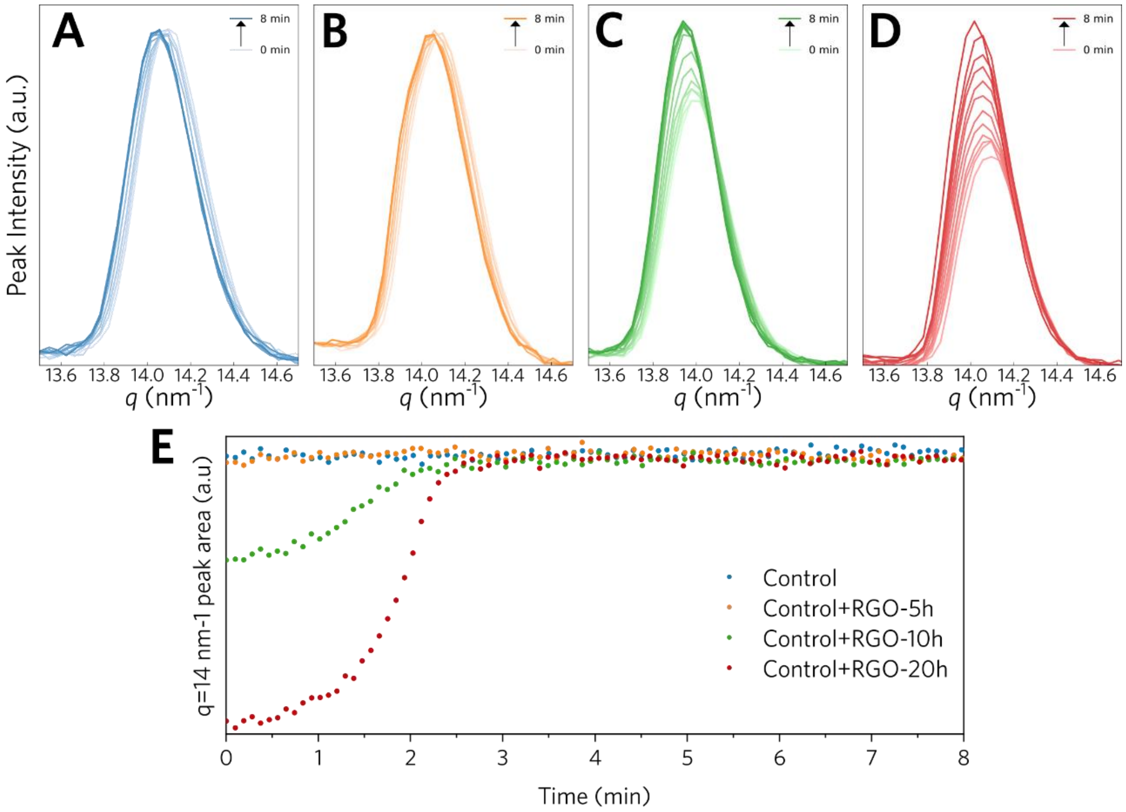

Figure S16: Area of q = 14 nm^{-1} peak over time.

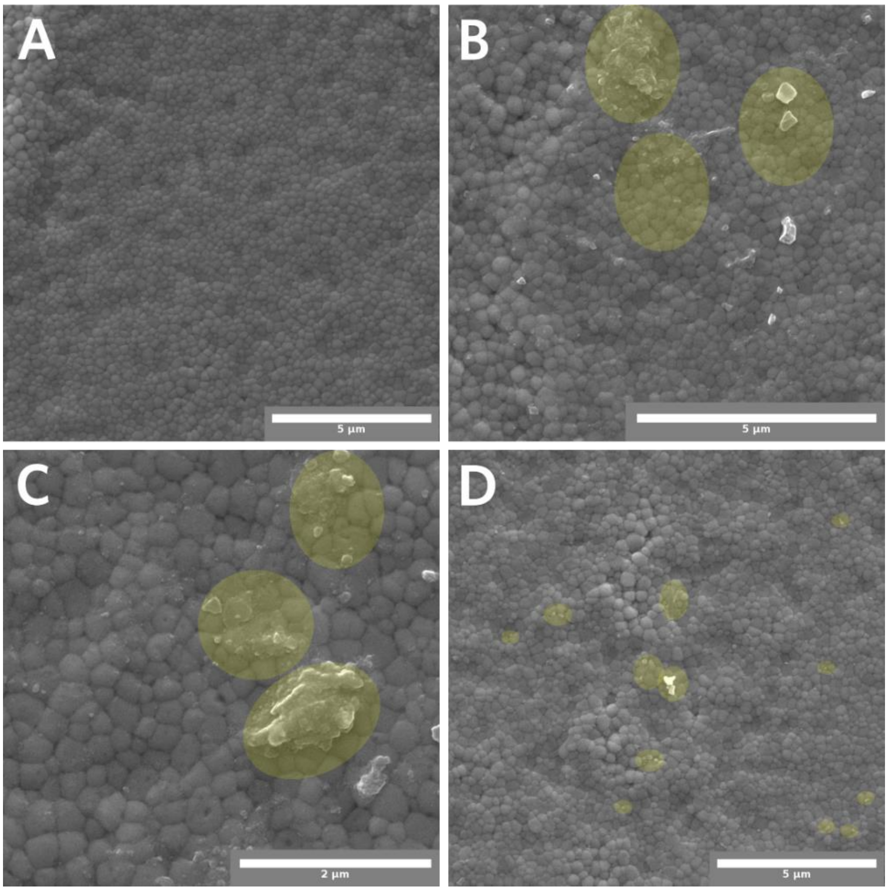

Figure S17: FEG-SEM images of the perovskite films prepared with precursors containing RGO. (A-D) Top view of Control, Control+RGO5h, Control+RGO10h, and Control+RGO20h samples, respectively. Yellow-marked regions regard the RGO in the perovskite films.

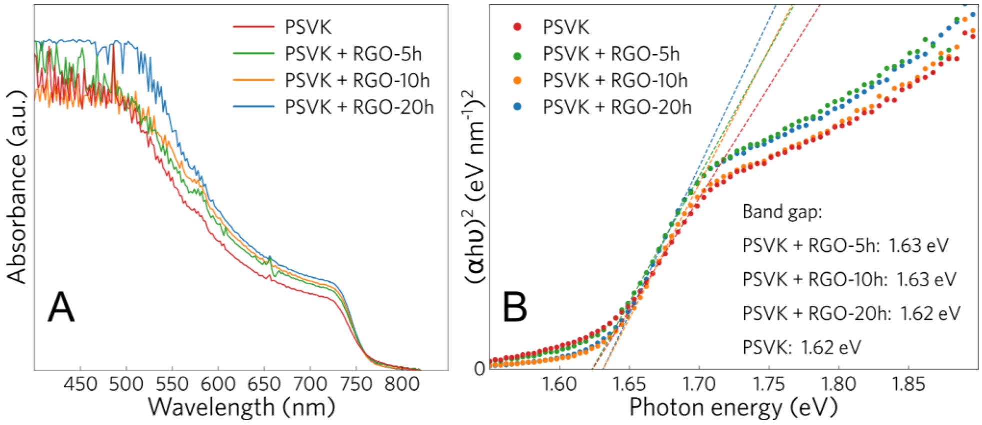

Figure S18: (a) UV-vis absorption spectra, (b) Tauc plots of samples PSVK, PSVK+RGO-5h, PSVK+RGO-10h and PSVK+RGO20-h.

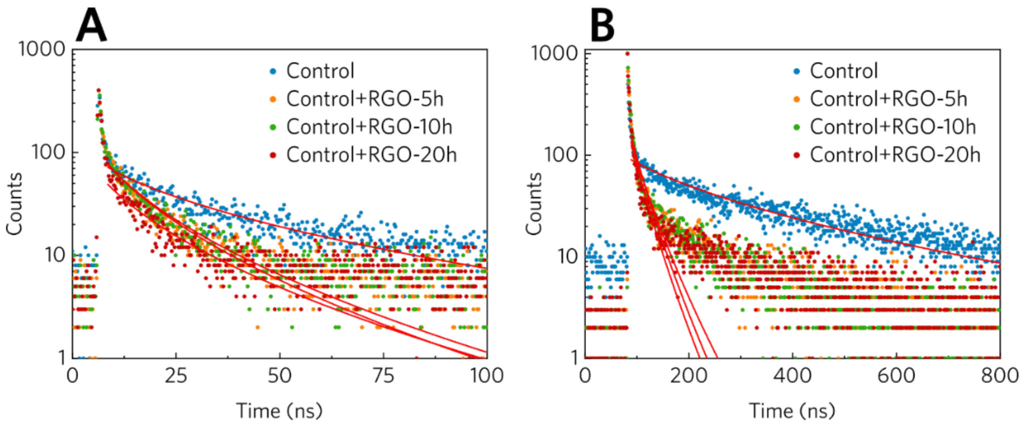

Figure S19: TrPL decays (λ_{PLE} = 445 nm; F = 24.3 nJ cm^{-2}; λ_{PL} = 755 nm) of the control 17/17 and RGO-modified films with a layer of Spiro-OMeTAD deposited on top of the perovskite film (a) and control 17/17 and RGO-modified films deposited onto a TiO_2-mp layer (b). Stretched exponential fit decays are shown in red curves.

Table S1: Charge-carrier lifetimes (τ_s) and disorder factor (β) for PSVK sample and RGO modified samples from TrPL experiments measured for samples deposited over a TiO_2-mp layer and with a layer of Spiro-OMeTAD deposited on top of the perovskite film.

	τ_s (ns)	β	R^2
	TiO_2-mp		
Control	65	0.5	0.85
Control +RGO-5h	1.8	0.5	0.80
Control +RGO-10h	1.4	0.5	0.82
Control +RGO-20h	1.2	0.5	0.77
	Spiro-OMeTAD		
Control	9.8	0.5	0.87
Control +RGO-5h	2.6	0.5	0.90
Control +RGO-10h	2.8	0.5	0.90
Control +RGO-20h	3.2	0.5	0.75

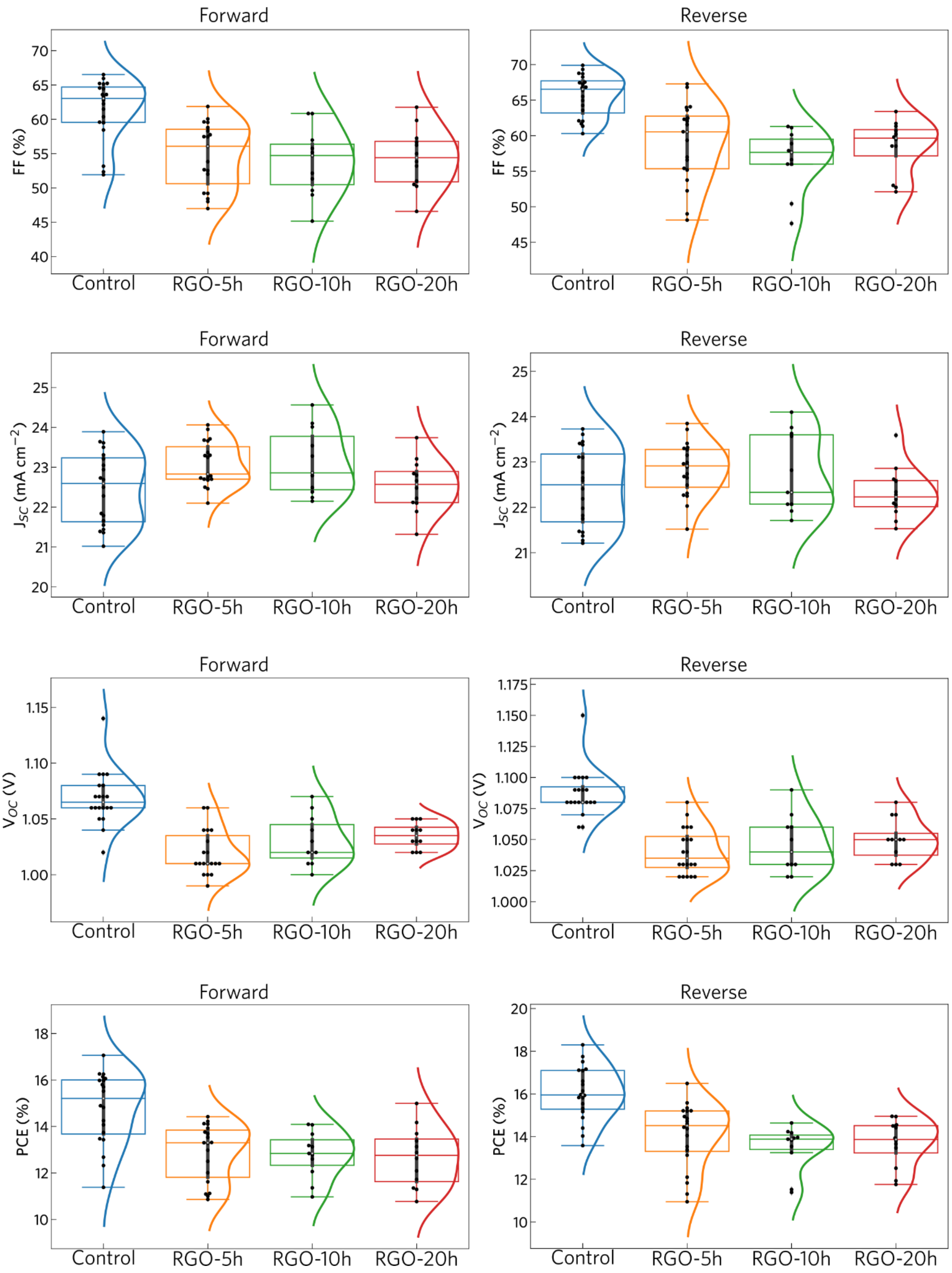

Figure S20: Statistical data of solar cells parameters as a function of reduction degree of RGO. (a,b) Forward and reverse FF, respectively; (c,d) Forward and reverse J_{SC}, respectively; (e,f) Forward and reverse V_{OC}, respectively; (g,h) Forward and reverse PCE, respectively.

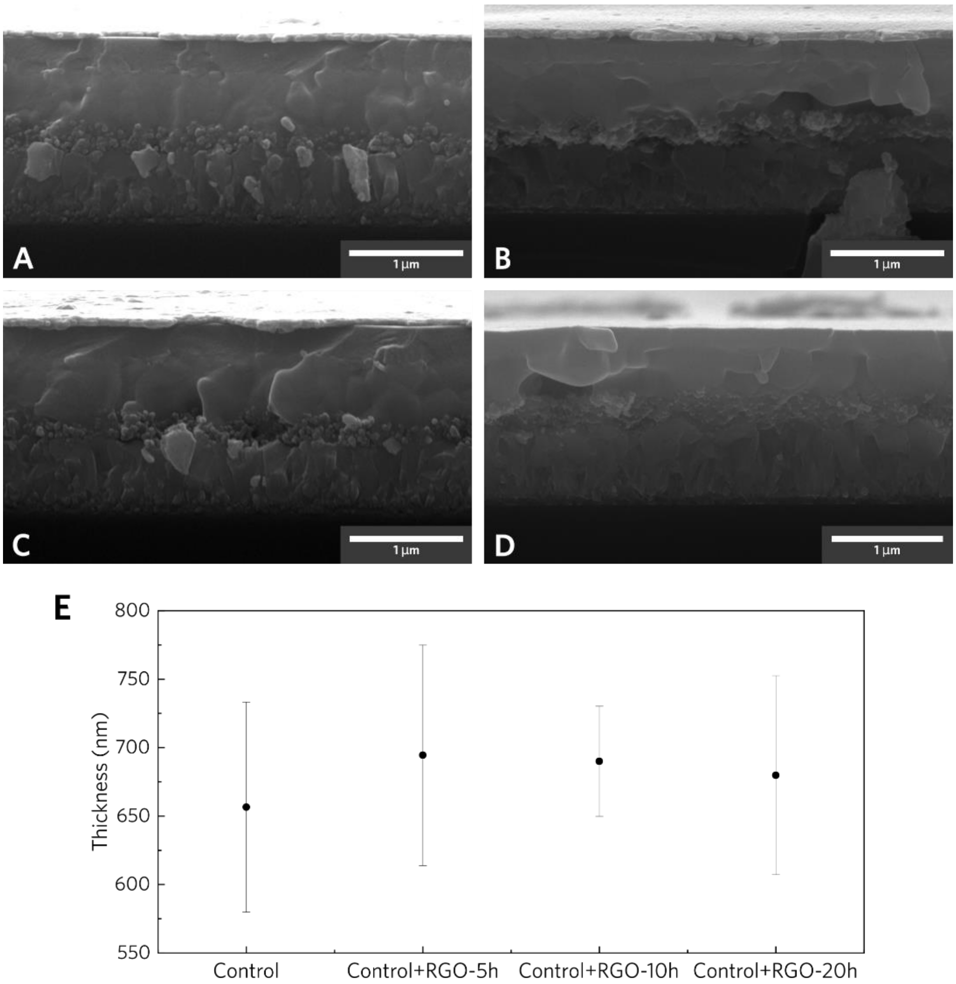

Figure S21: Cross section SEM images of the devices assembled for sample Control (A), Control+RGO-5h (B), Control+RGO-10h (C), Control+RGO-20h (D), and the average thickness for each sample (E).

Supplementary Text 1

The deconvolution of GO C 1s XPS core-level spectra (Figure S1b) consist of hydroxyl and epoxy groups (286.8 eV) and, to a lesser extent, quinone/carbonyl (288.5 eV) and carboxyl (290.0 eV) groups, in accordance with the Lerf-Klinowski model.[1] An increase in peak at binding energy of 284.5 eV, attributed to carbon with sp^2 hybridization, was observed in all RGO samples. The contribution of this peak to the total C 1s signal was 39% for RGO-5h, 45% for RGO-10h, and 47% for RGO-20h. Along with this change, a significant decrease in peaks associated with oxygenated carbons was observed for all RGO samples. Three main peaks were identified in the RGOs O 1s XPS core-level spectra (Figure S1c) that correspond to quinone (530.6 eV), oxygen double-bonded to carbon (532.5 eV), and oxygen single-bonded to carbon (533.7 eV). The O 1s XPS core-level for GO was composed with only two peaks, related to C=O (532.5 eV) and, mainly, C-O (533.7 eV). [2–6] A sharp decrease in the intensity of the peak at 533.7 eV reveals that oxygen single-bonded to carbon is preferentially removed upon hydrazine reaction, which is in agreement with the mechanism proposed by Stankovich *et al*.[7] These values suggest that the reaction with hydrazine not only promotes additional removal of oxygen but also improves restoration of sp^2 conjugation.

The appearance of nitrogen groups in RGO is evident and is due to the method chosen to reduce GO, which uses hydrazine.[8] The hydrazine introduces N atoms into RGO sheets. Three common bonding configurations within the carbon backbone are possible when nitrogen atoms are inserted into the graphene oxide sheet: pyrrolic N, pyridinic N, and graphitic N.[9] Pyrrolic-N refers to N atoms bond into the five-membered ring that share two p electrons with the π system. Pyridinic-N refers to nitrogen atoms at the edge of graphene planes; each of them is bonded to two carbon atoms and donates one p-electron to the aromatic π system. Graphitic N refers to N atoms that substitute C atoms in the hexagonal ring.[10] In our samples, the deconvolution of the high resolution N 1s XPS spectra (Figure S1d) shows that the N 1s peak can be resolved into three components centered at 399.4, 402.1, and 403.9 eV representing pyridinic, pyrrolic, and graphitic type of N atoms doped in the graphene structure, respectively. Accordingly, the pyrrolic N dominates in RGO samples prepared in this work.

Suplementary References

1 D. Chen, H. Zhang, Y. Liu and J. Li, *Energy Environ. Sci.*, 2013, **6**, 1362–1387.

2 Y. J. Oh, J. J. Yoo, Y. Il Kim, J. K. Yoon, H. N. Yoon, J. H. Kim and S. Bin Park, *Electrochim. Acta*, 2014, **116**, 118–128.

3 N. Díez, A.liwak, S. Gryglewicz, B. Grzyb and G. Gryglewicz, *RSC Adv.*, 2015, **5**, 81831–81837.

4 X. Fan, C. Yu, J. Yang, Z. Ling and J. Qiu, *Carbon N. Y.*, 2014, **70**, 130–141.

5 M. Hadadian, J.-P. Correa-Baena, E. K. Goharshadi, A. Ummadisingu, J.-Y. Seo, J. Luo, S. Gholipour, S. M. Zakeeruddin, M. Saliba, A. Abate, M. Grätzel and A. Hagfeldt, *Adv. Mater.*, 2016, **28**, 8681–8686.

6 Hui-Seon Kim, Bowen Yang, Minas M. Stylianakis, Emmanuel Kymakis, Shaik M. Zakeeruddin, Michael Grätzel, Anders Hagfeldt. *Cell Reports Phys. Sci.*, 2020, **1**, 100053.

7 S. Stankovich, D. A. Dikin, R. D. Piner, K. A. Kohlhaas, A. Kleinhammes, Y. Jia and Y. Wu, *Carbon N. Y.*, 2007, **45**, 1558.

8 X. Gao, J. Jang and S. Nagase, *J. Phys. Chem. C*, 2010, **114**, 832–842.

9 Z. Chen, W. Ren, L. Gao, B. Liu, S. Pei and H.-M. Cheng, *Nat. Mater.*, 2011, **10**, 424.

10 A. Reina, X. Jia, J. Ho, D. Nezich, H. Son, V. Bulovic, M. S. Dresselhaus and J. Kong, *Nano Lett.*, 2009, **9**, 30–5.